ASSESSMENT OF CRACK SHIELDING IN CERAMIC MATRIX COMPOSITES IN THE PRESENCE OF LARGE SCALE EFFECTS

Konstantinos G. Dassios[1] and Vassilis Kostopoulos[2]

[1] Mechanics of Materials Laboratory, Foundation for Research and Technology Hellas, Institute of Chemical Engineering and High Temperature Processes, P.O. Box 1414, Stadiou str., Platani, Patras GR-26504, Greece
[2] Department of Mechanical Engineering and Aeronautics, University of Patras, Rio GR-26504, Greece

ABSTRACT

A novel methodology is presented for assessing the macro-mechanics of large scale bridging in brittle-ceramic matrix composites. The principle of the methodology relies on the deconvolution of the recorded load-displacement behaviour of the composite into distinct contributions that include the contributions of the matrix, the intact/bridging fibres and the fibres that have failed and are undergoing pull-out. A model is presented for the assessment of the original force-displacement behaviour of SiC/MAS-L composites that utilizes the matrix, fibre and interface properties of the composite. The model makes use of appropriately coupled Weibull statistics to mathematically describe the effect of both the bridging and the pull-out mechanism to the load-carrying capacity of the composite and simulate their correlation. The fracture behaviour of the CFCC is analysed in terms of bridging laws and crack growth resistance using an elastic displacement correction approach for DEN specimens of different notch dimensions and thickness.

1. INTRODUCTION

Fracture in the vast majority of CFCCs is associated with the formation and propagation of macrocracks [1] within a confined damage area of the material, called the process zone. The process zone consists of two parts: the so called bridging zone with fibre bridging and pull-out developing within the macrocrack and a matrix cracking process zone ahead the macrocrack. The increase in fracture resistance is a result of several energy-dissipating mechanisms acting in the two zones. In the matrix process zone a complex set of phenomena such as matrix microcracking, fibre/matrix interfacial debonding and transformation toughening may take place concurrently. In the bridging zone the cracked matrix is bridged by intact and/or failed fibres, which debond, slip and pull-out. The role of the bridging zone in the fracture resistance of the composite is of particular importance as the bridging fibres carry a significant portion of the applied load, hence resisting further crack opening.

When the dimensions of the bridging zone are comparable to any specimen dimension -a phenomenon known as Large Scale Bridging (LSB) encountered in most CFCCs - the well established rising crack growth resistance with increasing crack extension behaviour of the composite (R-curve) is a material-extrinsic property which depends upon specimen geometry and dimensions [2,3]. Under LSB conditions, the fracture behaviour of CFCCs is preferably characterized by means of a bridging law, a local correlation between the stresses developing in the fibres within the bridging zone (bridging stresses) and the crack opening displacement (COD), i.e. the local opening of the crack flanks. The bridging law concept is a measure of the crack closure traction normalized to the local geometrical and dimensional characteristics of the material and, as such, has been proposed to serve as a basic, intrinsic, material law [4]. A number of studies have focused on the measurement of macromechanical bridging laws for composite materials mainly through the calculation of the bridging stress from the R-curve behaviour of the material [4-11]. Rouby et al [12] proposed a straightforward procedure for the macromechanical evaluation of bridging stresses and bridging laws in Double-Edge Notch (DEN) composite specimens based on the deconvolution of the load-displacement behaviour into an intact/bridging fibre and a pull-out fibre contribution.

In this study the macro-mechanics of large scale bridging are assessed through the analysis of tensile tests performed on double-edge notched (DEN) specimens of a SiC-fibre reinforced ceramic-glass matrix (MAS-L) composite material. The fracture behaviour of the CFCC is analysed in terms of bridging laws and crack growth resistance using an elastic displacement correction approach for DEN specimens of different notch dimensions and thickness.

A novel methodology is presented for the rationalization and quantitative assessment of real (experimental) bridging laws. The principle of the methodology is the deconvolution of the recorded bridging law into two distinct contributions: one corresponding to the intact/load-carrying fibres in the composite and one corresponding to the fibres undergoing pull-out. Under this principle, a theoretical model is developed for the assessment of the original force-displacement behaviour of composites exhibiting LSB that uses the matrix, fibre and interface properties of the composite. The formulation of the model includes the use of Weibull statistics for the mathematical description of the effect of both the bridging and the pull-out mechanism to the load-carrying capacity of the composite. One of the fundamental principles of the model relies on the appropriate coupling of the individual contributions to closely simulate the correlation that exists between the 2 mechanisms.

2. THEORETICAL BACKGROUND

Fibre Bridging Of Macrocracks

The mechanical behaviour of a fibre-bridged crack has been studied extensively in the past [13-16]. The Class I fracture characteristics (formation and development of a single macrocrack) of a brittle-matrix fibre-reinforced composite are presented in the load-displacement (F-d) behaviour of Fig. 1a whereas the mechanical processes occurring during testing are schematically depicted in Fig. 1b. During the initial loading stages, reversible mechanical phenomena occur within the composite (region O to A in Fig. 1a, stage 2 in Fig. 1b). The first matrix crack (point A in Fig. 1a) triggers the appearance of the bridging zone while cracking evolves (region A to B in Fig. 1a, stage 3 in Fig. 1b) until the macrocrack has fully developed, spanning the total width of the specimen (point B in Fig. 1a, stage 4 in Fig. 1b). Beyond this stage, fibres start failing within the volume of the composite and the load-carrying capacity of the remaining fibres decreases until a critical number of fibres have failed (point C in Fig. 1a). Failed fibres undergo pull-out and an additional contribution to the recorded load arises, owing to friction at the fibre/matrix interface (region B to D in Fig. 1a, stage 5 in Fig. 1b). Under the global load-sharing principle, each fibre failure is followed by a uniform redistribution of the remaining load to the surviving fibres. As the portion of load that corresponds to each intact fibre is greater after the redistribution, more failures are induced and the process evolves until all fibres have failed (point D in Fig. 1a). Beyond this stage, the load carried by the composite corresponds entirely to interfacial friction due to pull-out of failed fibres (region D to X in Fig. 1a, stage 6 in Fig. 1b). With increasing displacement, fibre ends that were originally located at various statistical locations inside the composite are sequentially disengaged from the matrix until, eventually, the composite separates in two parts.

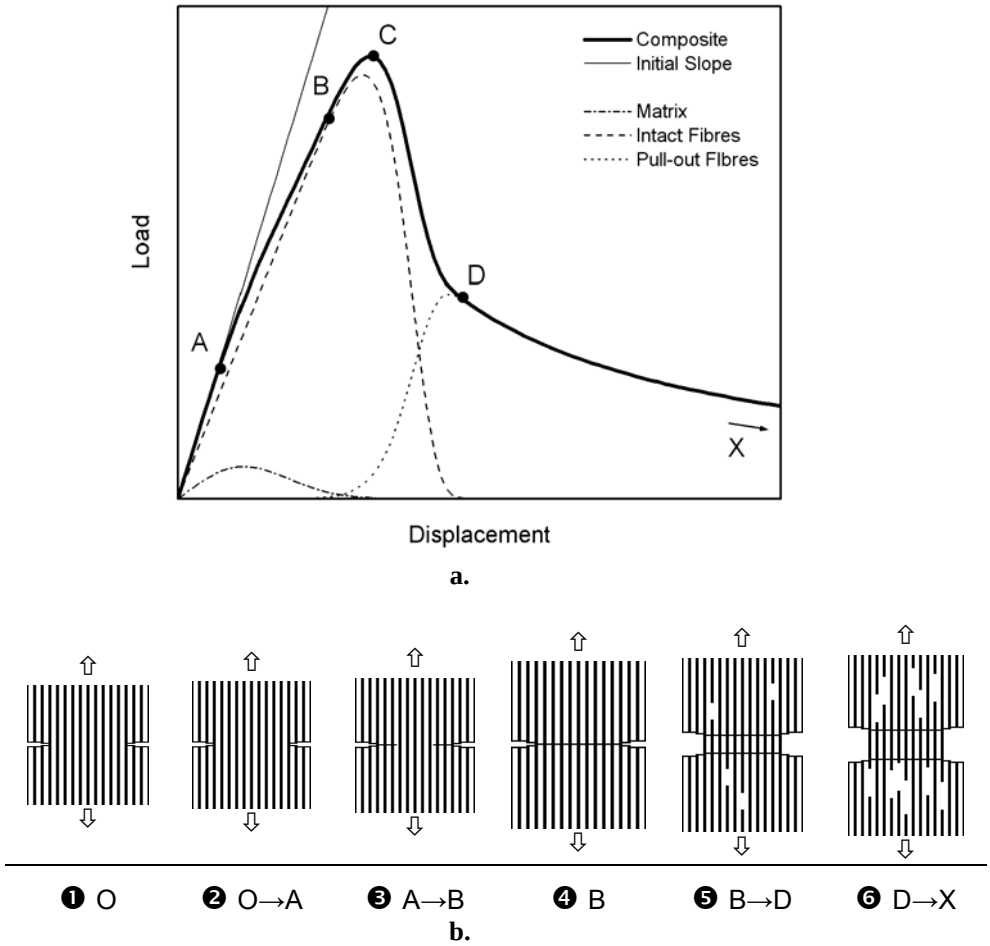

Fig. 1. a) Load-displacement (F-d) curve typical of Class I composite fracture and deconvolution of the curve into fibres- and matrix- contributions. b) Schematic overview of the main fracture processes in the composite.

Calculation of crack opening

In extension-controlled tests, the externally applied energy is consumed in reversible and irreversible phenomena and, accordingly, the total displacement is equal to the sum of a linear and a non-linear contribution. In Class-I fracture the non-linear part of the total displacement corresponds exclusively to crack opening, i.e. separation of the opposite sides of the macrocrack which, in turn, is always associated with the presence of a bridging zone. For example, in the regime beyond the fully developed macrocrack (beyond point B in Fig. 1a.), the load carried by a DEN specimen is equal to the load carried by the bridging (either intact or failed) fibres, F_{br}. Hence, the crack opening can be calculated by subtracting the elastic displacement of the system from the total recorded displacement, d. If D_0 is the initial slope of the measured load-displacement curve, the crack opening, $e(d)$, is obtained from the instantaneous load-displacement pairs (F,d) through:

$$e(d) = d - \frac{F(d)}{D_0} \tag{1}$$

Fig. 2 is a graphical illustration of the elastic displacement correction corresponding to Eq. (1).

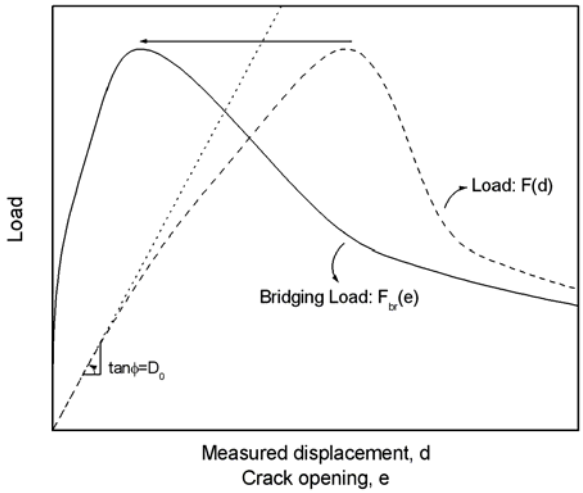

Fig. 2. Conversion of the measured load-displacement curve to a bridging load – crack opening curve using elastic displacement correction.

Crack growth resistance curve and bridging stresses

Accepting that non-linear contributions to the measured displacement stem directly from the presence of the bridging zone, the bridging work that contributes to the increase of crack opening resistance can be calculated as the area under the bridging stress versus crack opening curve (Fig. 3):

$$\Delta R = \Delta G = \int_0^e \frac{F_{br}(e)}{t \cdot (w - 2\alpha_0)} \cdot de \tag{2}$$

In Eq. (2), t is the specimen thickness, α_0 is the notch width and $t \cdot (w - 2\alpha_0)$ represents the area of the bridging zone, i.e. the cross section of the bridged ligament of the specimen. Accordingly, the integrand in Eq. (2) represents the nominal bridging stress, $\sigma_{br}(e)$.

$$\sigma_{br}(e) = \frac{F_{br}(e)}{t \cdot (w - 2\alpha_0)} \tag{3}$$

Eq. (3) represents the directly measured (real) bridging law.

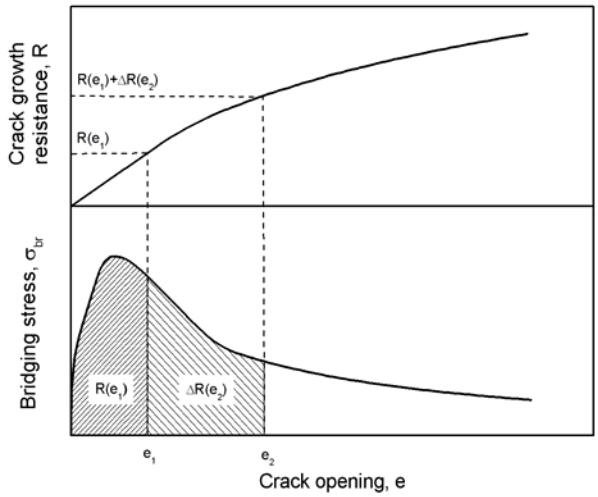

Fig. 3. DEN specimens: Evaluation of the R-curve from the bridging load - crack opening curve.

Model Formulation

The main principle behind the formulation of a model that assesses the load-displacement (P_{comp} - d) curve of the composite tested in axial tension is that, at every instance during testing, the total load carried by the composite can be expressed as the sum of three distinct contributions: the load contribution corresponding to the matrix, the load carried by intact fibres and the axial load due to sliding of pull-out (failed) fibres across the interface. The development of the model uses Weibull statistics principles and is presented analytically in [17]. The resultant modelled P_{comp} - d expression is given in Eq. 4.

$$P_{comp}(d) = \frac{A_{comp}(1-V_f)E_m}{L} \cdot d \cdot \exp\left[-\left(\frac{d}{d_{m,0}}\right)^{m_m}\right] + \frac{A_{comp}V_f E_f}{L} \cdot d \cdot \exp\left[-\left(\frac{d}{d_{f,0}}\right)^{m_f}\right] + \left(\frac{A_{comp}V_f \overline{l_p}}{r_f}\tau\right) \cdot \left\{1 - \exp\left[-\left(\frac{d-d_f^*}{d_{f,0}}\right)^{m_f}\right]\right\} \cdot \exp\left[-\frac{d-d_f^*}{d_p^*}\right] \quad (4)$$

where:

A_{comp} the cross sectional area of the composite

V_f the fibre volume fraction

E_m the elastic modulus of the matrix

L the gauge length over which d is measured

$d_{m,0}$ and m_m the Weibull parameters of the matrix

E_f the elastic modulus of the fibres

$d_{f,0}$, m_f the Weibull parameters of the fibres

$\overline{l_p}$ the mean pull-out length

τ the interfacial shear stress

r_f the fibre radius

d_p^* the pull-out extinction constant

d_f^* the displacement where the intact-fibre contribution deviates from linearity

3. MATERIALS, SPECIMENS and TESTING

The material used in this study is a laminated cross-ply SiC/MAS-L composite processed by EADS (ex-Aérospatiale, France). The reinforcing SiC fibres are grade Nicalon NL202 with a chemical composition in weight concentration terms of 56.6% Si, 31.7% C and 11.7% O.

The glass-ceramic matrix contains MgO, Al_2O_3, SiO_2 and LiO_2 and is made via the sol-gel route. Plates of 2.0 and 3.0 mm thickness with 8 and 12 plies respectively were produced via hot pressing. The laminae were stacked together in a symmetric $[0\text{-}90^o]_{2s}$ and $[0\text{-}90^o]_{3s}$ orientation for the 2.0 and 3.0 mm thick plate respectively. The effective volume fraction of the fibres in the loading direction is 0.17 [12] whereas the matrix stiffness (75 GPa) and failure strain are lower than the corresponding values for the fibre and hence cracks appear first in the matrix.

Double Edge Notch specimens of 2.0 and 3.0 mm thickness were machined from corresponding composite plates using a 150 μm thick diamond disk so that the external plies were oriented parallel to the tensile direction (0°). Specimens with 0.4, 0.5 and 0.6 initial

notch-to-width ratios were produced using a diamond disk of the same thickness while the specimen width, W, was 12 mm for the 2 mm thick specimens and 10 mm for the 3 mm thick specimens.

Mechanical testing under monotonic tensile loading conditions was performed in extension control on a MTS® 858 servo-hydraulic tabletop equipped with a 25 kN load cell under a constant crosshead velocity of 0.01 mm/min. Displacement was measured directly on the specimens by fixing a MTS® axial extensometer (gauge length 25 mm) to one side.

4. RESULTS & DISCUSSION

Eq. (4) was used to fit the experimental *P-d* curves. The regression was performed using the software "Origin" and convergence was achieved under the x^2 reduction criterion. Due to the large number of parameters in Eq. (4), many combinations of values may give the same result, especially for those entering as nominators or denominators in the same terms. Due to this fact and also in order to describe the fracture behaviour of the composite realistically, we have to i) input the values of some known parameters and ii) apply some logical conditions to the regression.

The gauge length L is a known quantity equal to the extensometer gauge length, 25 mm. The cross sectional area A_{comp} can be measured for each specimen. Furthermore, we also introduce V_f=0.34 and $\overline{l_p}$=690 μm [12] and r_f=7 μm. Because $\overline{l_p}$ and τ appear in the same term, the value of one of these parameters has to be introduced. Although there are reference values of τ, we chose to fix $\overline{l_p}$ and let τ be deduced because the experimental measurement of the mean pull-out length is a much more trivial, and thus less error-prone, task that the measurement of τ.

The conditions of the regression were taken with respect to displacement and are:

1. The matrix contribution cannot extend to displacements larger than the one that corresponds to the maximum load
2. The intact fibres contribution cannot extend to displacements that are associated with the tail region which is purely pull-out
3. The pull-out contribution should start at approximately the displacement were the fibre distribution deviates from linearity

Table 1 lists the statistical results of three regressions to equal in number experimental P-d curves of DEN specimens with different thicknesses and notch-to-width (length) ratios compared to the bibliographic values. Fig. 4 depicts the results of the regressions in a graphical form.

Using the modelled P-d curve of the DEN specimens and the same principles as in the elastic displacement correction methodology was followed for the test data, one can calculate the modelled form of the bridging laws and R-curves as well as the deconvoluted individual contributions of intact and failed fibres for both parameters. The results of this analysis are presented in Fig. 5 and 6.

Table 1. Statistical properties of regression output parameters

Parameter	*Mean, μ*	*St.Dev., σ*	*Variance, σ/μ*	*Reference*
Matrix elastic modulus, E_m [GPa]	69.5	5.62	8.08%	70[†]
Fibres elastic modulus, E_f [GPa]	207.9	16.82	8.09%	200[†]
Matrix Weibull modulus, m_μ [-]	1.889	0.0047	0.24%	-
Fibres Weibull modulus, m_f [-]	2.528	0.0100	0.39%	2.3-2.7[*]
Characteristic value for matrix, $d_{m,0}$ [mm]	0.0366	0.00210	5.73%	-
Characteristic value for fibres, $d_{f,0}$ [mm]	0.0952	0.00768	8.06%	-
Interfacial shear stress, τ [Mpa]	3.04	0.174	5.72%	2-5[‡]
Pull-out extinction constant, d_p^* [mm]	0.570	0.0569	9.98%	-
Pull-out appearance constant, d_f^* [mm]	0.0193	0.00041	2.12%	-
Extracted parameters				
Composite elastic modulus, E_{comp} [GPa]	117.9	9.54	8.09%	123[†]

The most important feature of the regressions is probably not the fact that they compare very well with the experimental data, as proven by Fig. 4, but rather the fact that the values of the output parameters remain practically constant between specimens with different bridging zone dimensions. While all values vary around the mean with a standard deviation of less than 10%, the most interesting result is the very small coefficient of variation of the interfacial shear stress (compared to the wide range of the bibliographic values). This remark, in conjunction with the fact that the model utilizes only material properties, proves that the modelled bridging law can serve as a material-intrinsic fracture descriptor.

The agreement between experimental and modelled *P-d* curves (and thus also of the extracted bridging laws and R-curves) implies that the model, Eq. (16), can assess realistically the fracture behaviour of the SiC/MAS-L composite. However, the use of the model as an *a priori* fracture prediction tool can be limited by the lack of knowledge of the values of some material properties.

5. CONCLUSIONS

In this study a novel rationale and a corresponding model is presented for the assessment of the macro-mechanics of large scale bridging in ceramic matrix composites. The principle of the methodology relies on the appropriate coupling of the distinct contributions of the matrix, the intact/bridging fibres and the pull-out fibres to the experimentally recorded load-displacement behaviour of the composite. The model makes use of Weibull statistics to mathematically describe the effect of both the bridging and the pull-out mechanism to the load-carrying capacity of the composite and simulate their correlation. The fracture behaviour of the CFCC is analysed in terms of bridging laws and crack growth resistance using an elastic displacement correction approach for DEN specimens of different notch dimensions and thickness. Given the small variance between the regressions performed on DEN specimens of different dimensions, it can be concluded that the modelled bridging law is independent of the specimen size and, thus, can be regarded as a material-intrinsic property for this type of composite system. Possibly -this will be investigated in the future- it can also serve as a material-intrinsic fracture descriptor for every composite exhibiting similar fracture characteristics as the investigated material (large scale bridging and pull-out).

[†] [18]
[*] [19]
[‡] [12]

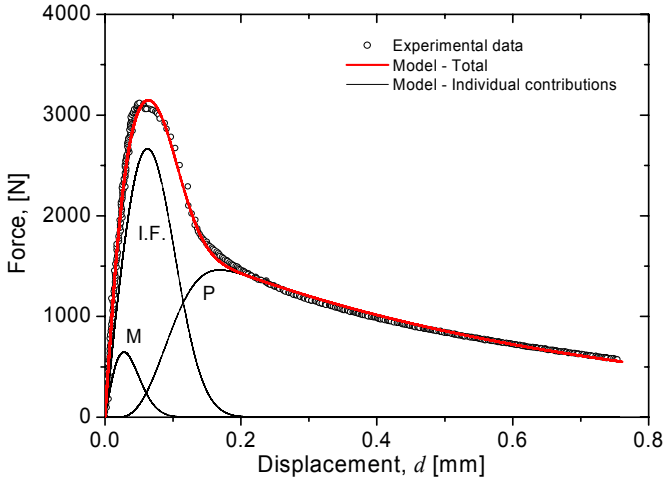

Specimen 1 (t=12.0 mm, W=12 mm, $2\alpha_0/W$=0.4)

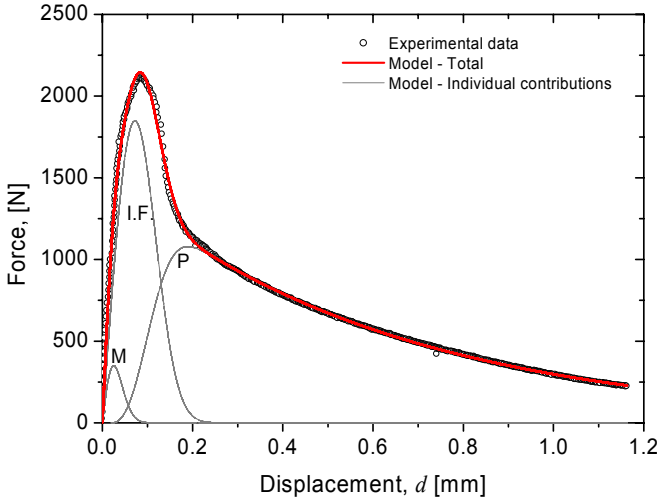

Specimen 2 (t=2.0 mm, W=12 mm, $2\alpha_0/W$=0.6)

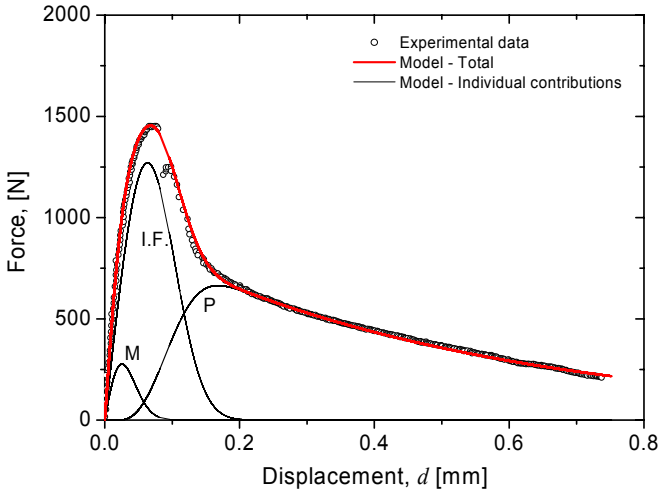

Specimen 3 (t=3.0 mm, W=10 mm, $2\alpha_0/W$=0.4)

Fig. 4. Experimental and theoretical P-d curves.
Abbreviations: M: Matrix contribution, I.F.: Intact fibres contribution, P: Pull-out fibres contribution

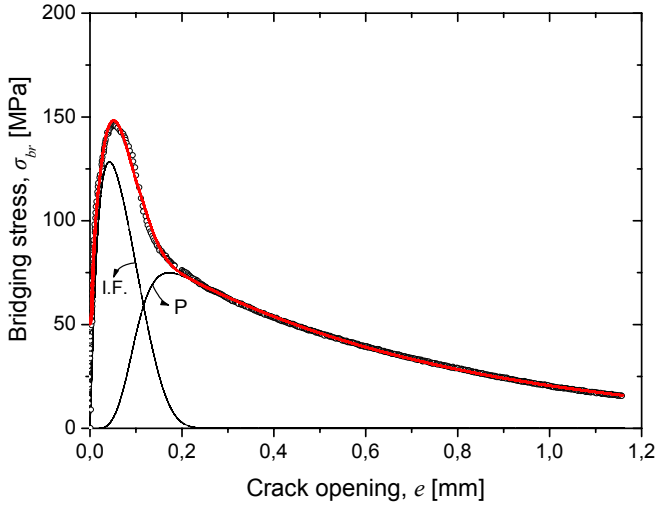

Fig. 5. Experimental and modelled bridging laws for specimen 3 (t=3.0 mm, W=10 mm, $2\alpha_0/W$=0.4)

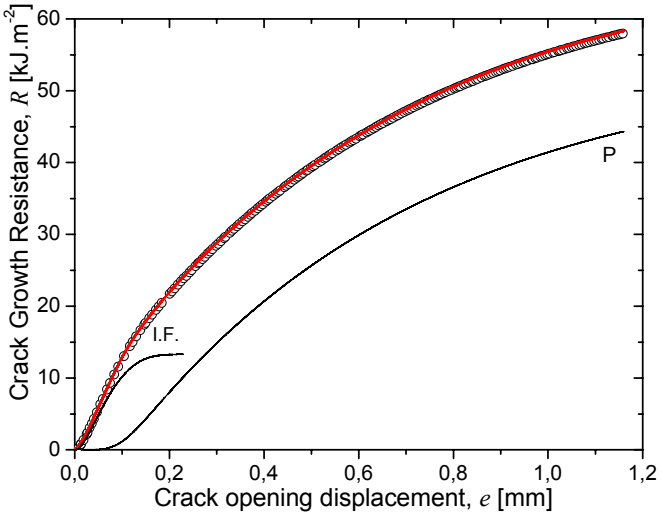

Fig. 6. Experimental and modelled R-curve for specimen 3 (t=3.0 mm, W=10 mm, $2\alpha_0/W$=0.4)

References

1. Evans, A.G. and Zok, F.W., *J. Mater. Sci.*, 1994, **29**, 3857.
2. Cox, B.N., *Acta Mater.*, 1991, **39**, 1189.
3. Fett, T., Munz, D. and Geraghty, R.D., White K.W., *Eng. Fract. Mech.,* 2000, **66**, 375.
4. Foote, R.M.L., Mai, Y-W., and Cotterell, B., *J. Mech. Phys. Solids*, 1986, **34**, 593.
5. Hu, X.Z. and Mai, Y.W., *J. Mater. Sci.*, 1992, **27**, 3502.
6. Fett, T. and Munz., D., *J. Eur. Ceram. Soc.,* 1995, **15**, 337.
7. Cao, J.W. and Sakai M., *Carbon,* 1996, **34**, 387.
8. Kostopoulos, V. and Markopoulos, Y.P., *Mat. Sci. Eng. A-Struct,* 1998, **250**, 303.
9. Sorensen, B.F. and Jacobsen, T.K., *Compos. Part A-Appl. S.,* 1998, **29**, 1443.
10. Rausch, G., Kuntz, M. and Gratwohl, G., *J. Am. Ceram. Soc.,* 2000, **84**, 2762.
11. Jacobsen, T.K. and Sorensen, B.F., *Compos. Part A-Appl. S.,* 2001, **32**, 1.
12. Brenet, P., Conchin, F., Fantozzi, G., Reynaud, P., Rouby, D. and Tallaron, C., *Compos. Sci. Technol.,* 1996, **84**, 817.
13. Dassios, K.G., Kostopoulos, V. and Steen, M., *Compos. Sci. Technol.*, 2003, in press.
14. Cox, B.N., Marshall, D.B. and Thouless, M.D., *Acta Mater.*, 1989, **37**, 1933.
15. Sutcu, M., *Acta Mater.*, 1989, **37**, 651.
16. Curtin, W.A., *J. Am. Ceram. Soc*., 1991, **74**, 2837.
17. Dassios, K.G., "Characterisation of the Fracture Behaviour of Ceramic Matrix Composites", PhD Thesis, University of Patras, Greece, July 2003
18. Drissi-Habti, M., 1997, *J. Eur. Ceram. Soc.*, **17**, 22.
19. Simon, G. and Bunsell, A.R., 1984, *J. Mater. Sci.*, **19**, 3649